Journal of Cerebral Blood Flow and Metabolism
21:1133–1145 © 2001 The International Society for Cerebral Blood Flow and Metabolism
Published by Lippincott Williams & Wilkins, Inc., Philadelphia

Review Article

An Energy Budget for Signaling in the Grey Matter of the Brain

David Attwell and *Simon B. Laughlin

*Department of Physiology, University College London, London, and *Department of Zoology, University of Cambridge, Cambridge, U.K.*

Summary: Anatomic and physiologic data are used to analyze the energy expenditure on different components of excitatory signaling in the grey matter of rodent brain. Action potentials and postsynaptic effects of glutamate are predicted to consume much of the energy (47% and 34%, respectively), with the resting potential consuming a smaller amount (13%), and glutamate recycling using only 3%. Energy usage depends strongly on action potential rate—an increase in activity of 1 action potential/cortical neuron/s will raise oxygen consumption by 145 mL/100 g grey matter/h. The energy expended on signaling is a large fraction of the total energy used by the brain; this favors the use of energy efficient neural codes and wiring patterns. Our estimates of energy usage predict the use of distributed codes, with ≤15% of neurons simultaneously active, to reduce energy consumption and allow greater computing power from a fixed number of neurons. Functional magnetic resonance imaging signals are likely to be dominated by changes in energy usage associated with synaptic currents and action potential propagation. **Key Words:** Action potential—Energy—fMRI—Resting potential—Signaling—Synapse.

The neural processing of information is metabolically expensive. Although the human brain is 2% of the body's weight, it accounts for 20% of its resting metabolism (Kety, 1957; Sokoloff, 1960; Rolfe and Brown, 1997). This requirement for metabolic energy has important implications for the brain's evolution and function. The availability of energy could limit brain size, particularly in primates (Aiello and Wheeler, 1995), and could determine a brain's circuitry and activity patterns by favoring metabolically efficient wiring patterns (Mitchison, 1992; Koulakov and Chklovskii, 2001) and neural codes (Levy and Baxter, 1996; Baddeley et al., 1997; Balasubramanian et al., 2001). The brain's energy requirements make it susceptible to damage during anoxia or ischemia, and understanding the demands made by different neural mechanisms may help the design of treatments (Ames et al., 1995). Interest in the relation between neural activity and energy use has been heightened by the development of functional imaging techniques. These techniques detect the mismatch between energy use and blood supply in small volumes of brain, and an increase in signal is taken to indicate heightened neural activity. However, with the exception of retina (Ames, 1992; Ames and Li, 1992; Ames et al. 1992; Laughlin et al., 1998), little is understood regarding the metabolic demands made by neural activity and the distribution of energy usage among identified neural mechanisms.

The restoration of the ion movements generated by postsynaptic currents, action potentials, and neurotransmitter uptake contributes to the brain's energy needs (Siesjö, 1978; Ames, 1992, 2000; Erecińska and Silver, 1989; Sokoloff et al., 1996). Excitatory synapses dominate the brain's grey matter (Abeles, 1991; Braitenberg and Schüz, 1998), and the distribution of mitochondria points to these glutamatergic synapses being major users of metabolic energy (Wong-Riley, 1989; Wong-Riley et al., 1998). Magnetic resonance studies (Sibson et al., 1998) find that glucose utilization is equal to the rate at which glutamate is converted to glutamine in the brain, which is a measure of synaptic glutamate release because the glia that take up glutamate convert some of it to glutamine. If the activity evoked by glutamate release is a major demand on brain energy supplies, then changes

Received May 1, 2001; final revision received July 17, 2001; accepted July 18, 2001.

Supported by the Wellcome Trust, the Rank Prize Fund, the BBSRC, and the Gatsby Foundation.

Address correspondence and reprint requests to David Attwell, Dept. Physiology, University College London, Gower St., London, WC1E 6BT, U.K.

in this glutamatergic activity may generate the imbalance between O_2 supply and metabolism that is detected as "activation" in functional magnetic resonance imaging experiments (Shulman and Rothman, 1998). However, glutamate release stimulates a number of mechanisms (for example, postsynaptic currents, action potentials, transmitter recycling) whose energy usage has not been systematically estimated.

This article uses anatomic and physiologic data from rodents (primates are discussed at the end of the article) to construct an energy budget for mammalian grey matter, specifying the metabolic cost of the mechanisms that generate and transmit neural signals. Taking advantage of biophysical data gathered in recent years, we derive the first reasonable estimates of the amounts of energy consumed by the major processes underlying neuronal signaling. These values specify the distribution of energy consumption between glia and neurons and between the neural mechanisms found in synapses, dendrites, and axons. The budget identifies major metabolic constraints to cortical function and, by specifying the dependence of energy usage on action potential frequency and synaptic transmission, will help to define the ability of functional imaging to detect changes in neural activity.

MATERIALS AND METHODS

Here, we present detailed calculations of energy expenditure on different cellular mechanisms in the brain. Readers who are interested in the conclusions of the analysis, but do not wish to go through the calculations in detail, can read the Results section with no loss of continuity. Limitations on the accuracy of the calculations are considered in the Discussion.

Energy needed for Na^+ extrusion

For a cell membrane with Na^+ and K^+ conductances (g_{Na} and g_K, with reversal potentials V_{Na} and V_K), and a pump that extrudes 3 Na^+ and imports 2 K^+ per adenosine triphosphate (ATP) consumed, on a time scale much slower than the membrane time constant, there is no net membrane current and

$$g_{Na}(V_{Na} - V) + g_K(V_K - V) = I_{pump} \quad (1)$$

where V is membrane potential, and the pump current, I_{pump}, is 1/3 of the Na^+ extrusion rate. Adenosine triphosphate is consumed at a rate I_{pump}/F (F is the Faraday). At the resting potential when $d[Na^+]_i/dt = d[K^+]_i/dt = 0$,

$$I_{pump} = g_{Na}(V_{Na} - V)/3 \quad (2)$$

From Eqs. 1 and 2, the current produced by Na^+ influx at the resting potential, V_{rp}, is

$$g_{Na}(V_{Na} - V_{rp}) = 3(V_{Na} - V_{rp})(V_{rp} - V_K)/\{R_{in}(V_{rp} + 2V_{Na} - 3V_K)\} \quad (3)$$

where the input resistance, R_{in}, is $1/(g_{Na}+g_K)$ and the rate of ATP consumption is

$$(V_{Na} - V_{rp})(V_{rp} - V_K)/\{FR_{in}(V_{rp} + 2V_{Na} - 3V_K)\} \quad (4)$$

When an action potential or synaptic current increases $[Na^+]_i$ and decreases $[K^+]_i$, the sodium pump will restore these concentrations, involving extra energy consumption. Rewriting Eq. 1 in terms of changes (Δ) from the resting values, the change of membrane potential is

$$\Delta V = (g_{Na}\Delta V_{Na} + g_K\Delta V_K - \Delta I_{pump})/(g_{Na} + g_K) \quad (5)$$

The rates of change of $[Na^+]_i$ and $[K^+]_i$ in a cell of volume U are

$$UF\, d[Na^+]_i/dt = g_{Na}(\Delta V_{Na} - \Delta V) - 3\Delta I_{pump} \quad (6)$$

$$UF\, d[K^+]_i/dt = g_K(\Delta V_K - \Delta V) + 2\Delta I_{pump} \quad (7)$$

From Eq. 5 – Eq. 7, $d[Na^+]_i/dt = -d[K^+]_i/dt$, and initially $\Delta[Na^+]_i = -\Delta[K^+]_i$ (when the membrane potential has returned essentially to its resting value, after an action potential or excitatory input, when the Na^+ entry has been balanced by K^+ exit). Thus, $\Delta[Na^+]_i = -\Delta[K^+]_i$ at all times. Equation 6 is solved by assuming that the pump rate varies linearly with small changes of $[Na^+]_i$ around the resting value so that

$$\Delta I_{pump} = \lambda\Delta[Na^+]_i \quad (8)$$

and using (for small concentration changes)

$$\Delta V_{Na} = -(RT/F)\ln([Na^+]_{i,new}/[Na^+]_{i,old}) \sim -(RT/F)(\Delta[Na^+]_i/Na_i);$$
$$\Delta V_K \sim -(RT/F)(\Delta[K^+]_i/K_i)$$

where Na_i and K_i are resting values. This gives (at time t)

$$\Delta[Na^+]_i(t) = \Delta[Na^+]_i(t = 0)\, e^{-t/\tau},$$

where

$$1/\tau = [\{g_{Na}g_K/(g_{Na} + g_K)\}\{RT/F\}\{(1/Na_i) + (1/K_i)\} + \lambda(2g_{Na} + 3g_K)/(g_{Na} + g_K)]/UF$$

The extra ATP consumed is

$$\int_0^\infty \Delta I_{pump}/F\, dt = \lambda\tau\, \Delta[Na^+]_i(t = 0)/F,$$

which is

$$(U\Delta[Na^+]_i(t = 0))/[\{g_{Na}g_K/(g_{Na} + g_K)\}\{RT/F\}\{(1/Na_i) + (1/K_i)\}/\lambda + (2g_{Na} + 3g_K)/(g_{Na} + g_K)] \quad (9)$$

If $g_{Na} \ll g_K$, and the sensitivity of the pump to $[Na^+]_i$ changes (λ) is large, this is ~(Na^+ load)/3, the approximation that is used in the rest of this article. In general, the ATP used differs from this value by an amount that depends on g_{Na}/g_K and λ. For the values of g_{Na}/g_K used below, $[Na^+]_i$ = 20 mmol/L, $[K^+]_i$ = 140 mmol/L, and a pump rate that depends on $[Na^+]_i$ according to a Hill equation with a Hill coefficient of 3 and an EC_{50} of 20 mmol/L, Eqs. 9, 8, and 2 show that for neurons and glia, respectively, the ATP used is 3% and 6% less than the value of (Na^+ load)/3. (The ATP usage can differ from (Na^+ load)/3 because we are calculating the change in usage from its resting value, and the increase in $[Na^+]_i$, decrease in $[K^+]_i$, and altered potential change the passive Na^+ influx, and hence the ATP needed to pump it out.) Other plausible $[Na^+]_i$ dependencies for the pump give similar small deviations from an ATP usage of (Na^+ load/3)—for example, 9% and 11% less, for neurons and glia, for a Hill coefficient of 2, or for a pump rate proportional to $[Na^+]_i$.

Energy needed for glutamatergic signaling

We consider the energy used (Fig. 1A) when 1 vesicle releases 4,000 molecules of glutamate (Riveros et al., 1986). Where necessary, reaction rates and ion channel conductances have been adjusted to 37°C using Q_{10} values of 3 and 1.3, respectively.

Glutamate recycling.

Glutamate uptake. Synaptically released glutamate is taken up mainly into astrocytes, driven by the cotransport with each glutamate of 3 Na^+ and 1 H^+, and the countertransport of 1 K^+ (Levy et al., 1998). For the Na^+/K^+ pump to transport back 3 Na^+ and 1 K^+, 1 ATP molecule is consumed. The H^+ will be pumped back by Na^+/H^+ exchange, requiring the extrusion of an extra Na^+ and consumption of 1/3 of an ATP. In total, 1.33 ATP molecules are consumed.

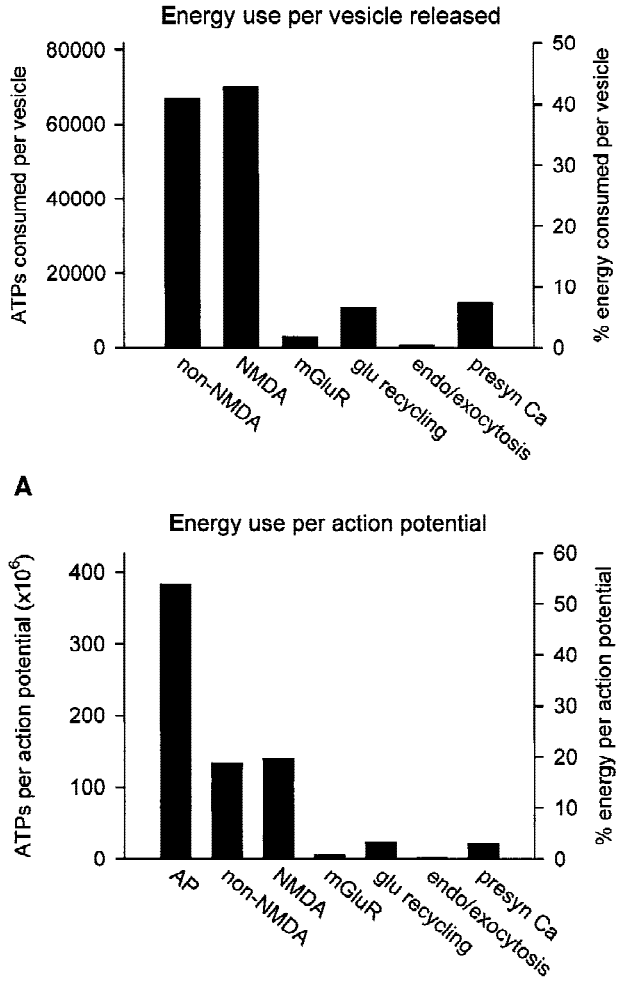

FIG. 1. Energy consumption of excitatory synaptic transmission and action potentials. **(A)** Adenosine triphosphate (ATP) usage produced by release of one vesicle of glutamate, calculated for the effects of glutamate on postsynaptic non–*N*-methyl-D-aspartate (non-NMDA), NMDA, and IP_3-linked metabotropic (mGluR) receptors, for uptake of glutamate, conversion to glutamine, and storage in vesicles (recycling), for the control of vesicle endocytosis and exocytosis, and for the presynaptic Ca^{2+} entry triggering vesicle release. **(B)** ATP usage produced by one action potential in a neuron, calculated for the voltage-gated currents producing the action potential (AP) and for the effects of glutamate release triggered by the action potential (other symbols as in **A**). Left axis, absolute ATP consumption; right axis, percentage consumption by the different cellular mechanisms.

Metabolic processing of glutamate. One third of the glutamate taken up is converted to glutamine (De Barry et al., 1983), a process requiring 1 ATP per glutamate, 1/4 of the glutamate remains as (or is converted back to) glutamate, 1/5 is converted to α-ketoglutarate by glutamate dehydrogenase, and the other 1/5 may be transaminated to aspartate. For simplicity, we assume that each of these pathways uses 1 ATP to process a glutamate.

Export of glutamine to neurons. Glutamine may leave glia and enter neurons on system N-like transporters (Chaudhry et al., 1999; Tamarappoo et al., 1997), which cotransport a Na^+ and countertransport a H^+ while consuming no energy (because the H^+ movement will be reversed by Na^+/H^+ exchange, which also reverses the Na^+ movement; the overall process is driven by the glutamine concentration gradient).

Packaging of glutamate into vesicles. This is powered by the vesicular H^+-ATPase. At least one H^+ is pumped to accumulate a glutamate anion, this minimum occurring if the vesicle membrane has negligible leak conductance. This requires hydrolysis of 1/3 of an ATP molecule, assuming the same H^+/ATP stoichiometry as for mitochondrial F-type ATPases. An extra 1.14 ATP/glutamate may be hydrolyzed to counteract leak (estimated from vesicular ATPase data (Wolosker et al., 1996) by assuming 100 seconds between successive releases of 1 vesicle); this would increase the total energy use per vesicle released (see below) by 3%.

Total energy to recycle glutamate. From the above, 2.67 ATP molecules are used to recycle each glutamate; consequently, for the 4,000 glutamate molecules in a vesicle, 11,000 ATPs are used.

Postsynaptic actions of glutamate.

*Ion fluxes through non–*N*-methyl-D-aspartate (non-NMDA) receptor channels.* At the cerebellar mossy fiber to granule cell synapse (Silver et al., 1996*a,b*), the hippocampal Schaffer collateral CA3-CA1 synapse (Jonas et al., 1993; Spruston et al., 1995), and excitatory synapses onto neocortical pyramidal cells (Hestrin, 1993; Markram et al., 1997; Häusser and Roth, 1997), release of a vesicle of glutamate leads to activation of 15, 30, and 15 to 200 postsynaptic non-NMDA channels, respectively (but the highest estimate was recognized as being perhaps more than 4-fold too high (Markram et al., 1997)), with a mean channel open time of 1, 0.6, and 1.4, milliseconds, respectively, and a channel conductance of 11.6, 12.6, and 13.3 pS (at 37°C), of which 2/3 is due to Na^+ for a reversal potential of 0 mV. If the driving force is $V_{Na} - V = 120$ mV, this gives an entry of 87,000, 96,000, and 140,000 to 1,867,000 Na^+, respectively (the last value being possibly more than 4-fold too high). As a weighted average, dominated by the more reliable values from noncortical neurons, we took 200,000 Na^+ entering. To pump these out, the Na^+/K^+ pump will hydrolyze approximately 67,000 ATP molecules.

Ion fluxes through NMDA receptor channels. NMDA channels have a higher conductance (50 pS) and longer open time (50 milliseconds) than non-NMDA channels, but are partly blocked by Mg^{2+} and are activated in fewer numbers by each vesicle of glutamate (as few as 2 channels in hippocampus (Spruston et al., 1995)). At cerebellar mossy fiber to granule cell synapses (Silver et al., 1992), hippocampal mossy fiber to CA3 cell synapses (Spruston et al., 1995), and synapses onto cortical pyramidal cells (Markram et al., 1997), the ratio of charge transfer through NMDA channels to that through non-NMDA channels is approximately 0.9, 2.0, and 0.15, respectively (assuming Mg^{2+}-block reduces NMDA receptor current

4.4-fold at −70 mV at cerebellar synapses (Jahr and Stevens, 1990)). Taking an average value of 1, and noting that 10% of the charge influx is carried by Ca^{2+} rather than Na^+ (Burnashev et al., 1995), this implies an entry of 180,000 Na^+ and 10,000 Ca^{2+} per vesicle of glutamate released. Each Ca^{2+} is extruded by 3 Na^+/Ca^{2+} exchange, leading to the entry of an extra 30,000 Na^+, so the total Na^+ entry is 210,000 ions requiring hydrolysis of 70,000 ATP molecules for their extrusion. Note that extrusion of Ca^{2+} by the plasma membrane Ca^{2+}-ATPase would use the same amount of ATP as $3Na^+/Ca^{2+}$ exchange.

Effects of glutamate on G protein–coupled receptors. Glutamate metabotropic receptors can activate phospholipase C to generate IP_3 and release Ca^{2+} from intracellular stores, alter cyclic adenosine monophosphate production, or inhibit Ca^{2+} channels. It is difficult to predict the energetic consequences of all these actions, but an estimate for phospholipase C–linked receptors can be made as follows. Activation of the mGluR1 receptors on one dendritic spine by the glutamate in one vesicle (assuming only one release site in the single synapse onto the spine (Harris and Stevens, 1988)) generates ~1 μmol/L IP_3 and releases sufficient Ca^{2+} to raise the free [Ca^{2+}] in the spine to ~1 μmol/L (Finch and Augustine, 1998). For a spine volume of 0.12 μm^3 (Harris and Stevens, 1988), and 39 out of every 40 added Ca^{2+} being buffered (Helmchen et al., 1997), then 72 IP_3 molecules and 2890 Ca^{2+} must be released in the spine. Each IP_3 molecule costs two ATPs to resynthesise, and for each Ca^{2+} an ATP must be hydrolyzed to pump the Ca^{2+} back into the endoplasmic reticulum. Assuming a much smaller ATP usage on G protein signaling, a total of approximately 3000 ATPs will be consumed.

Presynaptic Ca^{2+} fluxes and the vesicular release mechanism. The presynaptic action potential triggers an influx of 1.2×10^4 Ca^{2+} per vesicle released (at 35°C at calyx synapses (Helmchen et al., 1997)). This will be extruded by 3 Na^+/Ca^{2+} exchange, requiring 1.2×10^4 ATPs. The mechanics of exocytosis and vesicle recycling are poorly understood. The energy needed for membrane fusion has been estimated (Siegel, 1993), as that needed to form the "stalk" and "transmonolayer contact" structures postulated to lead to a fusion pore. This is ~200 kT, for lipid curvatures at the edge of the fusion region such that the "stalk" proceeds to a fusion pore, implying hydrolysis of 10.5 ATP molecules. If complete fusion of the vesicle and plasma membranes occurs, this will be needed for exocytosis and endocytosis, resulting in 21 ATP being consumed. Control of endocytosis by clathrin, adaptor proteins, dynamin, and hsc70 also uses ATP. Approximately 400 molecules/vesicle are involved (Marsh and McMahon, 1999), so if each were phosphorylated once, 400 ATPs/vesicle released are needed. The mechanisms that release the vesicle in response to Ca^{2+} presumably use a similar amount of energy and are not considered further.

Energy needed for action potentials

Neurons vary in their connectivity, but in rodent cortex, on average, action potentials propagate 4 cm from a neuronal soma through grey matter to synaptic terminals (Braitenberg and Schüz, 1998). This length is made up of numerous collaterals near the soma and in the axon termination zone, which in rodents are unmyelinated (Abeles, 1991; Braitenberg and Schüz, 1998). The short (~500 μm) myelinated part of the descending main axon and the axon in the white matter are not included in this analysis. A minimum Na^+ influx is needed to charge an axon to the peak of an action potential. Assuming a voltage change, $\Delta V = 100$ mV, a length of unmyelinated axon, $L = 4$ cm, of diameter, $d = 0.3$ μm (Braitenberg and Schüz, 1998), and capacitance, $C_m = 1$ μF/cm^2, needs an influx of $\pi dLC_m\Delta V = 3.77 \times 10^{-11}$ Coulombs, and this is provided by the entry of 2.36×10^8 Na^+ ions. The cell body also has to be depolarized by 100 mV; for a diameter, $D = 25$ μm, the minimum charge influx is $\pi D^2C_m\Delta V = 1.96 \times 10^{-12}$ Coulombs or 1.23×10^7 Na^+. Finally, the dendrites (3 times the diameter but 1/9 the length of the axon (Braitenberg and Schüz, 1998)) are polarized on average by 50 mV during an action potential (from simulations of cortical pyramidal cells by A. Roth and M. Häusser, as in Vetter et al., 2001) requiring entry of 3.93×10^7 Na^+. Thus, the minimum Na^+ influx to initiate the action potential and propagate it is 2.88×10^8 Na^+ (if dendrite depolarization were due to entry of Ca^{2+} instead of Na^+, with each Ca^{2+} extruded in exchange for 3 Na^+, this figure would increase by 6.8%). A realistic estimate of the Na^+ entry needed is obtained by quadrupling this to take account of simultaneous activation of Na^+ and K^+ channels (Hodgkin, 1975), resulting in 11.5×10^8 Na^+ which have to be pumped out again, requiring 3.84×10^8 ATP molecules to be hydrolyzed (Figs. 1B, 2, and 3). This 4-fold increase is validated by calculations by A. Roth and M. Hausser (as in Vetter et al., 2001), based on cell morphology and ionic current properties, which give ATP values of 3.3×10^8 for a cortical pyramidal cell with a myelinated axon, and 5.4×10^8 for a hippocampal pyramidal cell with an unmyelinated axon, similar to the estimate made above.

Energy expended on the resting potential

Neurons. For a neuron with a 200 MΩ input resistance (Hutcheon et al., 1996), and a −70 mV resting potential, generated by a K^+ conductance with $V_K = -100$mV and a smaller Na^+ conductance with $V_{Na} = +50$ mV, Eq. 4 shows that hydrolysis of 3.42×10^8 ATPs/s is needed to run the Na^+/K^+ pump to reverse the Na^+ entry and K^+ efflux (Figs. 2A and 3). *In vivo* recordings with sharp electrodes give input resistances less than 200 MΩ, but these may reflect more electrode damage and the tonic synaptic input that has already been accounted for in the estimates of energy usage on postsynaptic actions of transmitter.

Glia. Astrocyte steady-state input resistances range from 560 MΩ (probably single cells (Clark and Mobbs, 1994)) to 222 MΩ (possibly reduced by gap junctions with other cells (Bordey and Sontheimer, 1997)). As a weighted average, 500 MΩ was used. For $V_{rp} = -80$ mV (more negative than in neurons), $V_K = -100$ mV and $V_{Na} = 50$ mV. Equation 4 gives a usage of 1.02×10^8 ATP/cell/s (Fig. 2A).

Distributed coding, energy use, and coding sparseness

We consider a simple model of information coding to assess the impact of coding strategy on the energy consumption of the brain. To represent 100 different sensory or motor conditions, only one of which occurs at a time, the brain could use 100 neurons and have just 1 active at any one time to denote the particular condition occurring then. If R is the ATP usage per cell on the resting potential, and A is the extra ATP usage per cell on active signaling (action potentials plus glutamatergic signaling), then the total ATP used would be 100R + A. However, if a condition is represented by the simultaneous firing of 2 cells (at the same rate, with the others not firing), only 15 neurons are needed to represent 100 conditions (because 2 out of 15 neurons can be chosen in a number 15!/(13! 2!) = 105 different ways), and the energy expenditure is 15R + 2A. If R and A are equal (our budget suggests this is the case for neurons firing at 0.62 Hz), then this distributed representation gives a 6-fold reduction ((100R + A)/(15R + 2A) = 101/17) in energy usage for transmitting the same information. Similarly, if a condition is represented by 3 cells firing, only 10 cells are needed to represent 100 conditions (10!/(7! 3!) = 120), and the

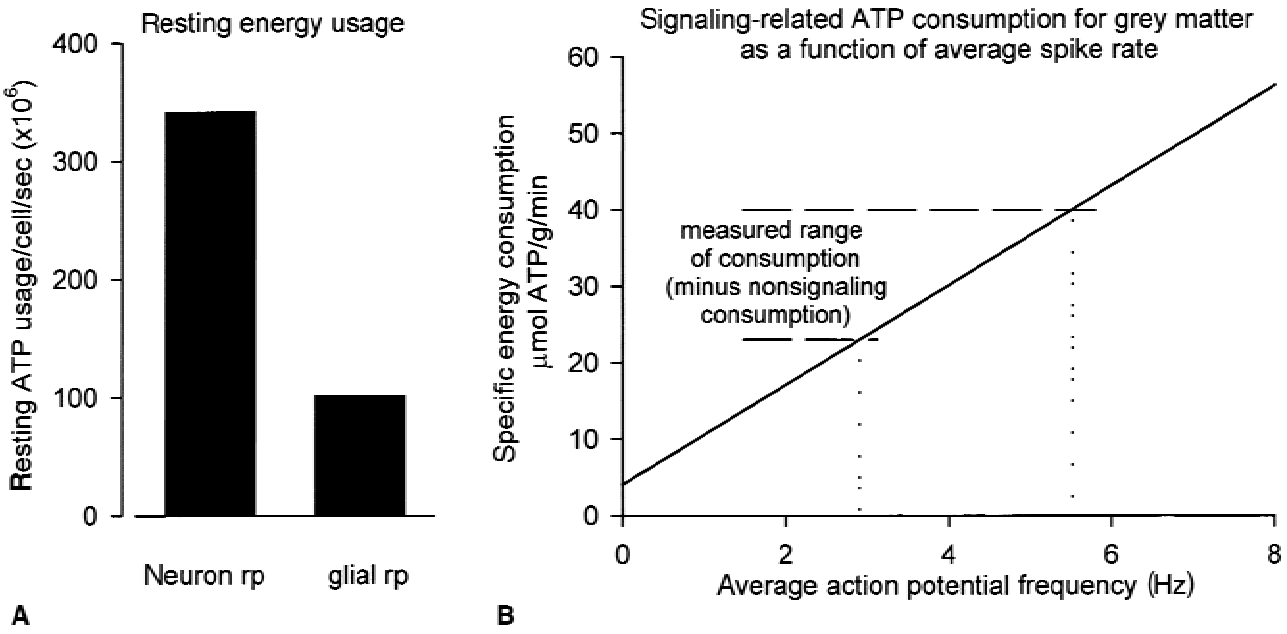

FIG. 2. Effect of spike activity on energy consumption. **(A)** Adenosine triphosphate (ATP) usage sustaining the resting potential (rp) of a neuron and glial cell. **(B)** Predicted effect of average action potential frequency on the specific signaling-related energy consumption of rodent grey matter (calculated from the ATP used per neuron as described in the text). At zero frequency, the usage is that sustaining the resting potentials shown in **A**. Dashed lines show the measured range of energy consumption in rat cortex (Clarke and Sokoloff, 1999) minus the estimated expenditure on nonsignaling activities (see Discussion).

energy expenditure is 10R + 3A, which (for R = A) is a further improvement of energy efficiency.

Figure 4A represents the energy used to encode a condition, as a function of the number of active neurons encoding the condition. The total number of neurons present is different for each number of neurons simultaneously active; it is set to allow the array of cells to represent 100 different conditions. Distributed coding gives a large reduction in the energy needed, and there is an optimum in the number of cells that should be active to encode a condition if the aim is to reduce energy expenditure (Levy and Baxter, 1996). For signaling by active cells at 0.62 Hz, this optimum is broad, with 3 (of 10) or 4 (of 9) cells simultaneously active to optimally encode a condition. If the system needs a higher temporal resolution, the active cells must fire at a higher rate, so that when a new condition occurs, the switch in identity of the cells firing will become detectable earlier. If active cells signal at 4 Hz, for which the calculations above give A = 6.4R, then the optimum becomes sharper and has just 2 cells (of 15) simultaneously active to optimally encode a condition. Finally, if active cells signal with action potentials at 40 Hz, for which the budget implies A = 64R, then the optimum becomes sharper still.

The sparseness of the optimal coding increases (that is, a smaller fraction of cells are simultaneously active) as the required temporal resolution (set by the action potential frequency) increases. To quantify this, calculations were performed like those in the previous paragraph for the encoding of either 100, 1000, or 10000 different conditions by a set of neurons. Figure 4B shows the energetically optimal fraction of simultaneously active cells, as a function of the action potential frequency used by the active cells.

RESULTS

To calculate the energy needs of various components of signaling in the brain, we analyze the transmitter release triggered by a single action potential passing through a typical neuron. As a simplification, all cells are treated as glutamatergic, because excitatory neurons outnumber inhibitory cells by a factor of 9 to 1, and 90% of synapses release glutamate (Abeles, 1991; Braitenberg and Schüz, 1998). From the number of vesicles of glutamate released per action potential, the number of postsynaptic receptors activated per vesicle released, the ion fluxes and metabolic consequences of activating a single receptor, and the energy costs of taking up and recycling transmitter glutamate, the energy needs of all the stages of glutamatergic signaling can be estimated. The next step is to compare the energy expended on the effects of glutamate to that needed for the action potential that triggers glutamate release and for maintenance of the resting potential between action potentials. By basing our calculations on the passage of signals through a single neuron, we obtained a clear picture of the relative amounts of energy used by different cellular processes and the relation between energy usage and action potential frequency. Finally, we multiply by the number of action potentials occurring in the neurons of a given brain volume to obtain the absolute energy expenditure. Comparison of these estimates with previously measured values tests the accuracy of the energy budget.

The analysis is based on values for rodent grey matter, for which the most data are available, but it is discussed at the end of the article how the conclusions differ for human brain. Data are taken largely from neocortex, particularly when scaling energy values by the number of

synapses and cells present, but when necessary data on synaptic properties are taken from other brain areas if they are more reliable than the data from neocortex. Although the individual energy values calculated here inevitably will be refined as more data become available, as discussed later, the distribution of energy usage among different mechanisms is unlikely to change significantly.

Details of the literature values used and the complete calculations are given in Materials and Methods. Here, we summarize the calculations and present the results.

Energy used to pump out Na^+ entering during signaling related processes

At rest, a cell with a membrane permeable to Na^+ and K^+ reaches an equilibrium with no net charge flux across the membrane, with Na^+ entry and K^+ exit through the membrane conductances exactly balanced by the pumped fluxes in the opposite directions, and with the ATP used by the Na^+/K^+ pump equal to 1/3 of the Na^+ entry through the membrane Na^+ conductance (see Materials and Methods, Eqs. 1 to 4). Action potential and synaptic signaling involve an influx of Na^+, and an equal efflux of K^+ to bring the membrane potential essentially back to its resting value. Our estimates of the ATP consumed by action potential and synaptic signaling depend on knowing how much extra ATP (above the resting consumption) is used to reverse these ion movements. To calculate this it is necessary to take into account the fact that the changes in ion concentrations and pump rate, which are evoked by signaling activity, alter slightly the membrane potential and the "resting" ion fluxes through the membrane conductances. As shown in Materials and Methods (Eqs. 5 to 9), the ATP used is determined by three factors: the ATP:Na^+:K^+ stoichiometry of the Na^+/K^+ pump, the ratio of the Na^+ to the K^+ conductance of the cell, and the $[Na^+]_i$-dependence of the pump. To within 3% to 10%, the ATP used is given by 1/3 of the Na^+ load that entered, an approximation that will be used throughout.

Energy required for signaling with one synaptic vesicle of glutamate

Signaling with one vesicle, containing approximately 4,000 molecules of glutamate (Riveros et al., 1986), requires energy to trigger the release of the vesicle, to power the postsynaptic events activated by the glutamate, and to recycle the vesicle and its glutamate. Of these, the major energy expenditure is on reversing the ion movements evoked by glutamate's actions on postsynaptic NMDA and non-NMDA ionotropic receptors, which together require hydrolysis of approximately 137,000 ATP molecules/vesicle (calculated in Materials and Methods from the number of channels activated per vesicle and their conductance, open time, and reversal potential). The energy usage resulting from activation of G protein–coupled receptors, including the generation of Ca^{2+} transients in spines, is more difficult to predict, but may be approximately 3,000 ATP molecules/vesicle (see Materials and Methods). This metabotropic receptor consumption is small because of the small volume of a spine and because the intracellular concentrations of second messengers are low. In total, the postsynaptic actions of a vesicle of glutamate are powered by the hydrolysis of 140,000 ATP molecules. In contrast, the recycling of 1 vesicle of glutamate uses 11,000 ATP molecules (see Materials and Methods), calculated from the energy needed to take glutamate up (mainly into astrocytes), convert it to glutamine, export it to neurons, and package it into vesicles. Finally, pumping out the Ca^{2+} influx that triggers vesicle release is estimated to consume 12,000 ATP molecules, and the as yet incompletely understood mechanisms of vesicle exocytosis and endocytosis may each consume another 400 ATPs.

Summing these estimates for presynaptic Ca^{2+} entry, vesicle cycling, postsynaptic actions, and glutamate recycling, the energy expended per vesicle of glutamate released is 1.64×10^5 ATP molecules. The distribution of energy use between the various synaptic mechanisms is shown in Fig. 1A. Postsynaptic ion fluxes dominate (84%). Presynaptic calcium influx and transmitter recycling are of secondary importance (7% each), and 2 elaborate molecular mechanisms, the metabotropic responses of spines and vesicle recycling, are a distant third (2% and 0.5%, respectively). This distribution reflects the fact that a chemical synapse is an amplifier: approximately 100 ions enter the postsynaptic terminal for each glutamate released. The energetic costs of recycling glutamate and vesicles are small because, despite the complexity of the mechanisms, the number of molecules involved is small.

Energy required to propagate an action potential

Vesicle release is triggered by action potentials, which are produced by ion movements that must be reversed. From the membrane area and capacitance that needs to be polarized, 1.15×10^9 Na^+ ions are required to propagate a single action potential through a typical neuron (see Materials and Methods). To pump out these ions requires hydrolysis of 3.84×10^8 ATP molecules. Of this amount, 82% supports action potential propagation to output synapses along axon collaterals, 14% supports depolarization of the dendrites, and 4% supports depolarization of the soma.

Comparison of the energy expended on action potential and glutamatergic signaling

Averaged over rodent neocortex, each action potential can evoke glutamate release from approximately 8,000 boutons (Braitenberg and Schüz, 1998). However, boutons do not always release a vesicle, and the release probability is dependent on action potential frequency.

At the climbing fiber synapse (Silver et al., 1998), the release probability (at 23°C) is 0.9 at low stimulus rates, but decreases to 0.15 at 4 Hz (the mean action potential frequency used below). Near 37°C in cortical neurons, the average release probability is 0.5 to 0.64 at low stimulation frequencies, and may be more than halved for frequencies greater than 5 Hz (Markram et al., 1997; Hardingham and Larkman, 1998). As an estimate for an action potential frequency of 4 Hz at 37°C, therefore, we took a release probability of 0.25, so that each action potential will release 2,000 vesicles from 8,000 boutons. From the results above, the energy expended on releasing one vesicle of glutamate (presynaptic Ca^{2+} entry, postsynaptic actions, glutamate recycling) is 1.64×10^5 ATP molecules, so these 2,000 vesicles have an energetic cost of 3.28×10^8 molecules of ATP, slightly less than the cost of the action potential that releases them (3.84×10^8 ATP). Thus, when a neuron fires an action potential, the total ATP consumption is 7.1×10^8 ATP/neuron/spike, most of which is expended on ion fluxes in axons and at synapses (Fig. 1B).

Energy expenditure on the neuronal and glial resting potentials

From their membrane potentials and input resistances, we calculated that 3.42×10^8 and 1.02×10^8 ATPs/s (Fig. 2A) are needed to maintain the resting potential of a typical neuron and glial cell (see Materials and Methods). In cortical grey matter, there are approximately the same number of glia as neurons (Haug, 1987), resulting in a total consumption of 4.44×10^8 ATPs/s per neuron (and associated glial cell). Because the ATP use triggered by each action potential is 1.6 times greater than this usage per second on the resting potentials, the total rate of energy consumption per neuron rises with spike rate from a low resting level (Fig. 2B), as found experimentally when increasing spike rate with electrical stimulation or decreasing it with anesthesia (Kety, 1957; Larrabee, 1958; Sokoloff, 1960; Ritchie, 1967; Lewis and Schuette, 1976; Sokoloff et al., 1977; Siesjö, 1978; Sibson et al., 1998; Clarke and Sokoloff, 1999).

Scaling energy consumption by action potential frequency

The mean firing rates of neurons in intact animals, engaged in natural patterns of behavior, are known only approximately. For freely moving rats, the rates of cortical units range from 0.15 to 16 Hz. The means, for neuronal populations in different areas and studies, range from 1.5 to 4 Hz (Schoenbaum et al., 1999; Fanselow and Nicolelis, 1999). Because these data were obtained in laboratories where sensory stimuli were controlled and limited, we took the upper value of mean rate, 4 Hz. Thus, for rodents, the ATP usage on signaling by action potentials and glutamate will be $4(3.84 \times 10^8 + 3.28 \times 10^8) = 2.85 \times 10^9$ ATPs/neuron/s. Adding the consumption on the resting potential gives a total rate of 3.29×10^9 ATPs/neuron/s at 4 Hz mean action potential frequency.

Distribution of energy usage

We have estimated that 3.42×10^8 ATPs/s are used to maintain the resting potential of a neuron, 1.02×10^8 per second to maintain the resting potential of associated glial cells, 15.4×10^8 per second are used for action potential signaling at 4 Hz in the neuron, and 13.0×10^8 per second are used for glutamatergic signaling from that neuron. These relations are shown in Fig. 3A. This distribution of energy usage is broadly reflected in the distribution of mitochondria (Fig. 3B). For visual cortex (Wong-Riley, 1989), 62% of mitochondria are in dendrites (we estimate 53% of brain energy is expended on the postsynaptic effects of glutamate, dendritic and somatic action potentials, and on the neuronal resting potential), 36% are in axons and presynaptic terminals (we predict that 42% of the energy goes on axonal action potentials, presynaptic Ca^{2+} entry, and accumulating glutamate into vesicles), and 2% are in glia (we predict that 5% of the energy goes on the glial resting potential, glutamate uptake and conversion to glutamine). Almost all of the energy usage that we have calculated goes on the Na^+/K^+ pump, to restore the ion gradients that generate electrical potentials.

Energy usage and specific rates of consumption of ATP, glucose, and oxygen

To convert from energy used per glutamatergic neuron to usage per gram of neocortical grey matter, we assume that all neurons are glutamatergic. This is a reasonable first step, because approximately 90% of cells and synapses are glutamatergic (Abeles, 1991; Braitenberg and Schüz, 1998); only if the 10% of nonglutamatergic neurons had a radically different pattern of energy use would the total usage or the distribution of usage over different cellular mechanisms be significantly affected. The activity of inhibitory neurons may lead to less postsynaptic energy use than the activity of excitatory neurons because, postsynaptically, Cl^- ions move down a smaller electrochemical gradient at inhibitory synapses than Na^+ ions do at excitatory synapses. As an extreme case, if it was assumed that inhibitory synapses use no energy at all on reversing postsynaptic Cl^- movements, the estimates (below) of total energy use per gram would decrease by 3%.

For a total ATP usage at a mean firing rate of 4 Hz of 3.29×10^9 ATPs/s/neuron, the 9.2×10^7 neurons/cm^3 (approximately per g) in the neocortex (Braitenberg and Schüz, 1998) will have a specific energy usage of 30 μmol ATP/g/min. This is similar to the rate of energy usage measured in rat grey matter, which is 33 to 50 μmol/g/min in different cortical areas (calculated from the observed glucose utilization of 107 to 162 μmol/100

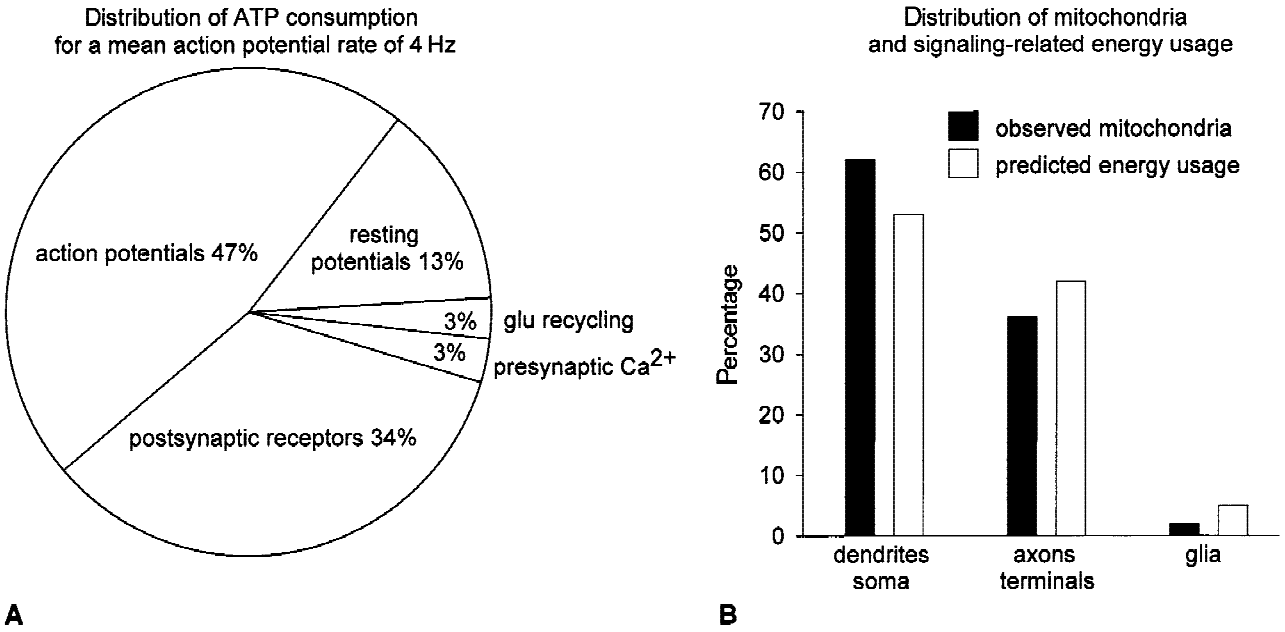

FIG. 3. (A) Distribution of signaling-related ATP usage among different cellular mechanisms when the mean firing rate of neurons is 4 Hz. The percentages of the expenditure maintaining resting potentials, propagating action potentials through a neuron, and driving presynaptic Ca^{2+} entry, glutamate recycling, and postsynaptic ion fluxes, are shown (100% = 3.29×10^9 ATP/neuron/s). **(B)** Comparison of our predicted distribution of signaling-related energy consumption with the distribution of mitochondria observed by Wong-Riley (1989). For the dendrites + soma column, Wong-Riley's data are the percentage of mitochondria in dendrites, whereas our prediction is the percentage of energy expended on postsynaptic currents, dendritic and somatic action potentials, and the neuronal resting potential. For the axons + terminals column, Wong-Riley's data are the percentage of mitochondria in axons and presynaptic terminals, and our prediction is for the percentage of energy expended on axonal action potentials, presynaptic Ca^{2+} entry, accumulating glutamate into vesicles, and recycling vesicles. The close spacing of terminals along axons (5 μm, implying a diffusion time of only 25 milliseconds (Braitenberg and Schüz, 1998)) will make terminal and axonal mitochondria functionally indistinguishable. For the glia column, Wong-Riley's data are the percentage of mitochondria in glia, whereas our prediction is for the energy expended on the glial resting potential, glutamate uptake, and its conversion to glutamine. This comparison ignores the 25% of energy expenditure not related to signaling (see Discussion), and the possibility that some processes (for example, in glia) may be driven mainly by glycolysis.

g/min (Sokoloff et al., 1977, tabulated in Clarke and Sokoloff, 1999) by assuming that, for glycolysis followed by oxidative phosphorylation, 31 ATP are produced per glucose (proton leak in mitochondria reduces the ATP/glucose ratio (Rolfe and Brown, 1997)). The estimate of 30 μmol ATP/g/min corresponds to an ATP consumption of 180 mmol/100 g/h, and thus (for 1 O_2 consumed per 6 ATP produced) an O_2 consumption of 30 mmol/100 g/h, or 670 mL at standard temperature and pressure, similar to the measured cortical O_2 consumption of unanesthetized rats, that is, 600 mL/100 g/h (Baughman et al., 1990). We conclude that a major fraction of the energy used by the brain's grey matter goes on signaling-related processes. The energy used by nonsignaling processes is considered in the Discussion.

Of the total ATP and O_2 used on signaling, 86.5% (that expended on action potentials and glutamatergic signaling) will scale with action potential frequency if changes in release probability and postsynaptic response with frequency are ignored. As a rule of thumb, 1 spike/neuron/s equates to the consumption of 6.5 μmol ATP/g grey matter/min (which is 16% of the total ATP consumption of grey matter, which is 40 μmol ATP/g/min, see Discussion), or 21 μmol glucose/100 g/min, or to an O_2 consumption of 145 mL/100 g/h.

Energy consumption in primate brain

The above calculations used values for rodent brain, which require adjustment for comparison with data on human brain. Few data are available to calculate the postsynaptic ion fluxes activated by a glutamatergic vesicle in humans. Action potential–related energy usage may be increased by a greater axon and dendrite length (Abeles, 1991) for at least some neurons in the larger brain, and by the higher mean firing frequency (perhaps 9 Hz rather than 4 Hz) in primates (Baddeley et al., 1997), but will be decreased by the lower vesicle release probability at the higher frequency. More major changes in the predicted energy budget of the brain will result from the 3- to 10-fold lower density of neurons (Abeles, 1991) in humans, with an unchanged density of synapses, implying a 3- to 10-fold higher number of synapses/neuron. For a 10-fold change, this will increase the fraction of ATP usage devoted to reversing the postsynaptic effects of glutamate (from 34% to approximately 74%), but will reduce by 54% the specific

energy usage and O_2 consumption to approximately 14 μmol ATP/g/min and 308 mL O_2/100g/min. Interestingly, metabolic rates in neocortical grey matter are indeed, on average, 54% lower in monkey than in rat (Sokoloff et al., 1977; Kennedy et al., 1978; tabulated in Clarke and Sokoloff, 1999).

High energy usage of the brain favors distributed coding

For some parts of the nervous system, the number of neurons and energy expenditure needed are dictated by the type of information processed—for example, the number of retinal ganglion cells is set by the required spatial resolution. At higher levels of the nervous system, the representation of information can be more abstract, and distributed coding, in which a piece of information is represented as the simultaneous activity of a number of neurons rather than the firing of a single neuron, offers economies of energy usage. The optimal distribution of activity depends on the relative amounts of ATP used to support the resting potential and to support active signaling (Levy and Baxter, 1996). In Materials and Methods, for a simple model of information coding, we calculate the most energy economical way for the brain to represent a certain number of conceptual categories or sensorimotor conditions, and then use the energy consumption values derived above to predict how sparse the coding used should be for different values of mean action potential frequency (corresponding loosely to different levels of temporal resolution, see Materials and Methods).

The results in Fig. 4A show that for active cells signaling at 4 Hz, distributed coding offers a 4-fold reduction in energy usage when encoding 100 different conditions. The energy saving rises to 200-fold when encoding 10,000 different conditions (not shown). It only becomes energetically favorable to have the activity of a single cell encoding a condition at very high firing rates (greater than 60 Hz when encoding 100 different conditions, and greater than 600 Hz for 1000 conditions). The fraction of neurons simultaneously active is predicted to decrease when higher temporal resolution is needed (Fig. 4B). For an action potential frequency of 4 Hz in active cells, approximately 15% of a set of neurons should be simultaneously active to encode a condition, with a weak dependence on the number of different conditions (from 100 to 10000) being encoded by the set of neurons, whereas at greater than 10 Hz, a smaller fraction of cells should be active. Thus, sparse coding is not only computationally advantageous (Marr, 1969; Olshausen and Field, 1996), but saves energy as well (Levy and Baxter, 1996).

DISCUSSION

Based on published anatomic and physiologic data from rodents, we have estimated the energy expenditure on different aspects of information processing by the grey matter of the rodent brain. This analysis suggests a definite hierarchy of energy usage (Fig. 3A). Most demanding are action potentials and postsynaptic potentials (47% and 34% of total signaling-related usage for action

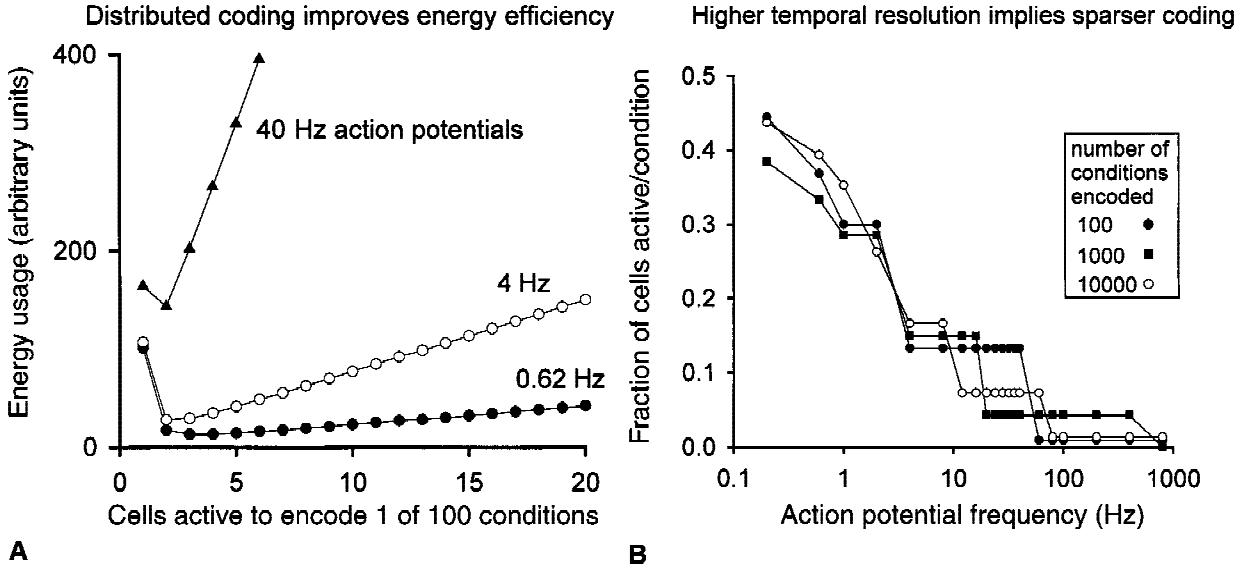

FIG. 4. Reducing energy usage with distributed coding. **(A)** Energy usage to encode 1 of 100 different conditions, as a function of the number of cells simultaneously active to denote one condition (firing action potentials at the frequencies shown), based on our calculated energy consumption values. **(B)** Energetically optimal value for the fraction of cells active to encode a condition (at the minima of curves as in **A**), as a function of action potential frequency in active cells (the average firing rate of the cell ensemble is given by the frequency in active cells multiplied by the fraction of cells active—for example, 40 Hz in active cells with 10% of cells active results in an average rate of 4 Hz). Each curve is for a different total number of distinct encodable conditions (100, 1000, 10000).

potential firing at 4 Hz), second are neuronal and glial resting potentials (13%), presynaptic calcium entry and neurotransmitter recycling are third (each 3%), and least demanding are calcium transients in spines and vesicle recycling (<1%). To carry out this analysis it is obviously necessary to make greatly simplifying assumptions, such as treating all neurons as identical. It is inevitable, therefore, that these estimates of energy usage will change somewhat as better and more detailed data become available (the major uncertainties are described below). Nevertheless, the large differences predicted for the different cellular mechanisms, and the fact that these differences stem largely from the different numbers of ions or molecules involved in each process, suggest that the hierarchy in Fig. 3A is robust. Notable is the large fraction of the signaling energy budget devoted to action potentials (47%), which is in stark contrast to an earlier estimate (0.3% to 3%) based on heat production (Creutzfeldt, 1975).

Brain grey matter has a higher energy usage (33 to 50 μmol ATP/g/min in neocortex) than that of the whole brain (21 μmol ATP/g/min), probably because of the high signaling-related energy demand in grey matter (Sokoloff et al., 1977; Kennedy et al., 1978; Siesjö, 1978; Rolfe and Brown, 1997; Clarke and Sokoloff, 1999). For the whole brain, or for brain slices containing grey and white matter, blocking the Na/K pump (on which essentially all of the energy in our budget is expended) or inducing coma approximately halves the energy usage (Kety, 1957; Sokoloff, 1960; Siesjö, 1978; Astrup et al., 1981; Ames, 1992, 2000; Rolfe and Brown, 1997), leaving a residual energy consumption of ~10 μmol ATP/g/min. This presumably sustains basic cellular activities that are not tightly coupled to signaling, such as the turnover of macromolecules (proteins, oligonucleotides, lipids), axoplasmic transport, and mitochondrial proton leak. In rat brain, protein synthesis consumes approximately 0.4 μmol ATP/g/min, which is only 2% of the brain's total ATP consumption. This hydrolysis rate is calculated from a protein turnover in whole rat brain of 0.6%/h and a protein content of 100 mg/g (Dunlop et al., 1994), by assuming that 4 ATP molecules are required to form a peptide bond with an average molar weight of 110 (Rolfe and Brown, 1997). It is generally considered that the turnover of oligonucleotides and lipids uses less energy than protein synthesis (Ames, 1992, 2000; Clarke and Sokoloff, 1999), but the contribution of phospholipid metabolism may have been underestimated. Recent discoveries of high rates of phospholipid turnover, and the use of energy to maintain asymmetrical distributions of phospholipids in membrane bilayers, suggest that phospholipid metabolism could consume 1 μmol ATP/g/min (Purdon and Rapoport, 1998). This usage constitutes approximately 5% of the total rate for whole brain given above (21 μmol ATP/g/minute). The energy consumed by axoplasmic transport has not been determined (Ames, 2000). Proton leak in mitochondria (independent of ATP generation) has not been addressed in brain but accounts for 20% of the resting energy consumption in a variety of tissues (Rolfe and Brown, 1997).

Assuming that white and grey matter expend similar amounts of energy on these basic (nonsignaling) cellular activities, ~10 μmol ATP/g/minute, our total predicted energy usage in rodent grey matter increases from the signaling-related 30 μmol ATP/g/min calculated above to a total of 40 μmol ATP/g/min. This is in the middle of the measured range of energy consumption in rodent grey matter (33 to 50 μmol ATP/g/min) (Clarke and Sokoloff, 1999). Conversely, subtracting 10 μmol ATP/g/min from this measured range of values gives a predicted use on signaling of 23 to 40 μmol ATP/g/min (Fig. 2B), similar to our prediction of 30 μmol ATP/g/min. These figures suggest that 75% of energy expenditure in grey matter is devoted to signaling, consistent with the large decrease of energy use produced by anesthesia (Kety, 1957; Sokoloff, 1960; Siesjö, 1978; Sibson et al., 1998; Clarke and Sokoloff, 1999).

Our estimates are subject to a number of uncertainties, the most important of which are as follows. First, the synaptic conductance is a major determinant of the energy expended on synaptic transmission, but literature values for neocortical neurons vary by more than a factor of 10 so we have constrained the value chosen using more reliable data from nonneocortical synapses (see Materials and Methods). Second, in estimating the mean action potential frequency of neurons at 4 Hz, there is concern that some classes of neuron (particularly those that fire rarely) are undersampled. Third, in calculating the energy expended on action potential and synaptic use, we have assumed that action potentials invade all the branches of an axon, but branch point failure may prevent invasion of some branches. Finally, the estimate of the energy used by the very fine axons present in grey matter is derived by scaling values for larger axons by the relative membrane area in small axons, and it is possible that the underlying ionic currents differ significantly in smaller axons.

Because the factors we considered account for a major fraction of the brain's energy use, we have demonstrated that it is feasible to construct energy budgets from the bottom up, using known neuronal properties. This success suggests the merit of a broader study that relates regional differences in energy usage to differences in neuronal structure and function. We have shown that a decrease in cell density with no change in synapse density greatly elevates the relative importance of synaptic costs in primate brain. It remains to be seen how changes in cell and synapse density and mean firing rate account for the 1.5-fold variation of metabolic rates between cortical areas and for the differential effect of anesthetics on

energy use in different brain areas (Sokoloff et al., 1977; Siesjö, 1978; Clarke and Sokoloff, 1999). For example, the synaptic energy cost is high but is proportional to two parameters: the probability that an action potential releases transmitter at a bouton, and the number of postsynaptic channels activated by transmitter. The literature values of these two parameters vary, suggesting that they could be adjusted to minimize the power consumption of particular cortical circuits. Currently, however, there are insufficient data available to estimate the energy consumption of particular brain areas.

The energy budget confirms that brain is, by the nature of its work, "expensive tissue" (Aiello and Wheeler, 1995). The signaling-related energy use of 30 μmol ATP/g/min is equal to that in human leg muscle running the marathon (Hochachka, 1994). Such a high metabolic rate will limit the brain's size (Aiello and Wheeler, 1995) and favor mechanisms that use energy efficiently (Sarpeshkar, 1998). With most of the energy being used to drive ion pumps, any factor that reduces ionic fluxes without reducing information content and processing power improves energy efficiency. Reducing the number of active synapses and ion channels to just greater than the level where synaptic and channel noise starts to destroy information, by fine tuning the properties of membranes, synapses, and circuits, is beneficial. Such tuning must take temporal resolution into account. Higher temporal resolution requires a higher action potential frequency and a lower membrane time constant (so that synaptic currents can produce fast rising potentials), both of which require a high energy expenditure (indeed, metabolic rates are 40% greater in auditory areas (Sokoloff et al., 1977; Kennedy et al., 1978; tabulated in Clarke and Sokoloff, 1999)). The brain has adapted to constraints on energy usage by using distributed codes (Levy and Baxter, 1996), which greatly reduce the energy needed to represent and transmit information (Fig. 4), by using economical wiring patterns (Mitchison, 1992; Koulakov and Chklovskii, 2001) and by eliminating unnecessary signal components (for example, many neurons respond transiently, which reduces information redundancy and hence the number of spikes used for a given task). The energy budget shows that such economy is essential in the neocortex. An increase in mean firing rate of 1 Hz increases consumption (in rodent) by 6.5 μmol ATP/g/min, so that a mean firing rate of 18 Hz for all neurons would increase consumption to the maximum (120 μmol ATP/g/min (Hochachka, 1994)) that can be sustained by human muscle. This modest mean rate would compromise both the construction and the size of the neocortex by requiring a considerable expansion of the vasculature.

Functional magnetic resonance imaging signals have been suggested to reflect the level of glutamatergic synaptic transmission (Shulman and Rothman, 1998). Data showing equality of the rate of glucose consumption and of glutamine formation in the brain were interpreted (Sibson et al., 1998) to imply that glutamatergic activity is the major energy drain on the brain, and that energy use on glutamate uptake and conversion to glutamine was likely to control glucose usage and cortical blood flow. The estimates above show that energy expenditure on glutamatergic signaling is indeed significant, approximately 34% of the total signaling energy usage going on glutamate postsynaptic actions in rodents and perhaps 74% in humans. However, the energy expended on glutamate uptake and glutamine synthesis is only 2% of the signaling-related total (in rodents, 5% in humans). Thus, if functional magnetic resonance imaging signals simply reflect total energy expenditure, they will be determined primarily by glutamate's postsynaptic actions and the ion currents underlying action potentials (Fig. 3A), both of which are very sensitive to the spike rate (Fig. 2B).

Acknowledgments: The authors thank Arnd Roth and Michael Häusser for carrying out action potential simulations, Adelbert Ames III, Roland Baddeley, Michael Häusser, Leon Lagnado, Mart Mojet, Maria Ron, Arnd Roth, and Angus Silver for helpful discussion, and Jonathan Ashmore, Céline Auger, Brian Burton, Gonzalo Garcia de Polavieja, Martine Hamann, and Peter Mobbs for comments on the manuscript.

REFERENCES

Abeles M (1991) *Corticonics: neural circuits of the cerebral cortex.* Cambridge: CUP

Aiello LC, Wheeler P (1995) The expensive tissue hypothesis: the brain and the digestive system in human and primate evolution. *Curr Anthropol* 36:199–221

Ames A 3rd (1992) Energy requirements of CNS cells as related to their function and to their vulnerability to ischemia: a commentary based on studies on retina. *Can J Physiol Pharmacol* 70:S158-S164

Ames A 3rd, Li YY (1992) Energy-requirements of glutamatergic pathways in rabbit retina. *J Neurosci* 12:4234–4242

Ames A 3rd, Li YY, Heher EC, Kimble CR (1992) Energy-metabolism of rabbit retina as related to function: high cost of Na^+ transport. *J Neurosci* 12:840–853

Ames A 3rd, Maynard KI, Kaplan S (1995) Protection against CNS ischemia by temporary interruption of function-related processes of neurons. *J Cereb Blood Flow Metab* 15:433–439

Ames A 3rd (2000) CNS energy metabolism related to function. *Brain Res Rev* 34:42–68

Astrup J, Sorensen PM, Sorensen HR (1981) Oxygen and glucose consumption related to Na^+-K^+ transport in canine brain. *Stroke* 12:726–730

Baddeley R, Abbott LF, Booth MCA, Sengpiel F, Freeman T, Wakeman EA, Rolls ET (1997) Responses of neurons in primary and inferior temporal visual cortices to natural scenes. *Proc R Soc Lond B* 264:1775–1783

Balasubramanian V, Kimber D, Berry MJ 3rd (2001) Metabolically efficient information processing. *Neural Comp* 13:799–815

Baughman VL, Hoffman WE, Miletich DJ, Albrecht, RF (1990) Cerebrovascular and cerebral metabolic effects of N_2O in unrestrained rats. *Anesthesiology* 73:269–272

Bordey A, Sontheimer H (1997) Postnatal development of ionic currents in rat hippocampal astrocytes *in situ*. *J Neurophysiol* 78:461–477

Braitenberg V, Schüz A (1998) *Cortex: statistics and geometry of neuronal connectivity, 2nd ed.* Berlin: Springer

Burnashev N, Zhou Z, Neher E, Sakmann B (1995) Fractional calcium currents through recombinant glutamate receptor channels of the NMDA, AMPA and kainate receptor subtypes. *J Physiol* 485:403–418

Chaudhry FA, Reimer RJ, Krizaj D, Barber D, Storm-Mathisen J, Copenhagen DR, Edwards RH (1999) Molecular analysis of system N suggests novel physiological roles in nitrogen metabolism and synaptic transmission. *Cell* 99:769–780

Clark BA, Mobbs P (1994) Voltage-gated currents in rabbit retinal astrocytes. *Eur J Neurosci* 6:1406–1414

Clarke JB, Sokoloff L (1999) Circulation and energy metabolism of the brain. In: *Basic neurochemistry, 6th ed.* (Siegel GJ, Agranoff BW, Albers RW, Fisher SK, Uhler MD, eds), Philadelphia: Lippincott-Raven, pp 637–669

Creutzfeldt OD (1975) Neurophysiological correlates of different functional states of the brain. In: *Alfred Benzon Symposium VII* (Ingvar DH, Lassen NA, eds), New York: Academic Press, pp 21–46

De Barry J, Vincendon G, Gombos G (1983) Uptake and metabolism of L-[^{3}H] glutamate and L-[^{3}H]glutamine in adult rat cerebellar slices. *Neurochem Res* 8:1321–1335

Dunlop DS, Yang XR, Lajtha A (1994) The effect of elevated plasma phenylalanine levels on protein synthesis rates in adult-rat brain. *Biochem J* 302:601–610

Erecińska M, Silver IA (1989) ATP and brain function. *J Cereb Blood Flow Metab* 9:2–19

Fanselow EE, Nicolelis MAL (1999) Behavioral modulation of tactile responses in the rat somatosensory system. *J Neurosci* 19:7603–7616

Finch EA, Augustine GJ (1998) Local calcium signalling by inositol-1,4,5-trisphosphate in Purkinje cell dendrites. *Nature* 396:753–756

Hardingham NR, Larkman AU (1998) The reliability of excitatory synaptic transmission in slices of rat visual cortex *in vitro* is temperature dependent. *J Physiol* 507:249–256

Harris KM, Stevens JK (1988) Dendritic spines of rat cerebellar Purkinje cells: serial electron microscopy with reference to their biophysical characteristics. *J Neurosci* 8:4455–4469

Haug H (1987) Brain sizes, surfaces, and neuronal sizes of the cortex cerebri: a stereological investigation of man and his variability and a comparison with some mammals (primates, whales, marsupials, insectivores, and one elephant). *Am J Anat* 180:126–142

Häusser M, Roth A (1997) Estimating the time course of the excitatory synaptic conductance in neocortical pyramidal cells using a novel voltage jump method. *J Neurosci* 17:7606–7625

Helmchen F, Borst JG, Sakmann B (1997) Calcium dynamics associated with a single action potential in a CNS presynaptic terminal. *Biophys J* 72:1458–1471

Hestrin S (1993) Different glutamate receptor channels mediate fast excitatory synaptic currents in inhibitory and excitatory cortical neurons. *Neuron* 11:1083–1091

Hochachka PW (1994) *Muscles as molecular and metabolic machines.* Boca Raton: CRC Press

Hodgkin AL (1975) The optimal density of sodium channels in an unmyelinated nerve. *Phil Trans Roy Soc Lond* 270:297–300

Hutcheon B, Miura RM, Puil E (1996) Models of subthreshold membrane resonance in neocortical neurons. *J Neurophysiol* 76:698–714

Jahr CE, Stevens CF (1990) Voltage dependence of NMDA-activated macroscopic conductances predicted by single-channel kinetics. *J Neurosci* 10:3178–3182

Jonas P, Major G, Sakmann B (1993) Quantal components of unitary EPSCs at the mossy fiber synapse on CA3 pyramidal cells of rat hippocampus. *J Physiol* 472:615–663

Kennedy C, Sakurada O, Shinohara M, Jehle J, Sokoloff L (1978) Local cerebral glucose utilization in the normal conscious macaque monkey. *Ann Neurol* 4:293–301

Kety SS (1957) The general metabolism of the brain *in vivo.* In: *Metabolism of the nervous system* (Richter D, ed), London: Pergamon, pp 221–237

Koulakov AA, Chklovskii DB (2001) Orientation preference patterns in mammalian visual cortex: a wire length minimization approach. *Neuron* 29:519–527

Larrabee MG (1958) Oxygen consumption of excised sympathetic ganglia at rest and in activity. *J Neurochem* 2:81–101

Laughlin SB, de Ruyter van Steveninck RR, Anderson JC (1998) The metabolic cost of neural information. *Nat Neurosci* 1:36–41

Levy LM, Warr O, Attwell D (1998) Stoichiometry of the glial glutamate transporter GLT-1 expressed inducibly in a CHO cell line selected for low endogenous Na^+-dependent glutamate uptake. *J Neurosci* 18:9620–9628

Levy WB, Baxter RA (1996) Energy efficient neural codes. *Neural Comp* 8:531–543

Lewis DV, Schuette WH (1976) NADH fluorescence, $[K^+]_o$ and oxygen consumption in cat cerebral cortex during cortical stimulation. *Brain Res* 110:523–535

Markram H, Lubke J, Frotscher M, Roth A, Sakmann B (1997) Physiology and anatomy of synaptic connections between thick tufted pyramidal neurones in the developing rat neocortex. *J Physiol* 500:409–440

Marr D (1969) A theory of cerebellar cortex. *J Physiol* 202:437–470

Marsh M, McMahon HT (1999) The structural era of endocytosis. *Science* 285:215–220

Mitchison G (1992) Axonal trees and cortical architecture. *Trends Neurosci* 15:122–126

Olshausen BA, Field DJ (1996) Emergence of simple-cell receptive field properties by learning a sparse code for natural images. *Nature* 381:607–609

Purdon AD, Rapoport SI (1998) Energy requirements for two aspects of phospholipid metabolism in mammalian brain. *Biochem J* 335:313–318

Ritchie JM (1967) The oxygen consumption of mammalian nonmyelinated nerve fibers at rest and during activity. *J Physiol* 188:309–329

Riveros N, Fiedler J, Lagos N, Munoz C, Orrego F (1986) Glutamate in rat brain cortex synaptic vesicles: influence of the vesicle isolation procedure. *Brain Res* 386:405–408

Rolfe DFS, Brown GC (1997) Cellular energy utilization and molecular origin of standard metabolic rate in mammals. *Physiol Rev* 77:731–758

Sarpeshkar R (1998) Analog versus digital: extrapolating from electronics to neurobiology. *Neural Comput* 10:1601–1638

Schoenbaum G, Chiba AA, Gallagher M (1999) Neural encoding in orbitofrontal cortex and basolateral amygdala during olfactory discrimination learning. *J Neurosci* 19:1876–1884

Shulman RG, Rothman DL (1998) Interpreting functional imaging studies in terms of neurotransmitter cycling. *Proc Natl Acad Sci U S A* 95:11993–11998

Sibson NR, DhankarA, Mason GF, Rothman DL, Behar KL, Shulman RG (1998) Stoichiometric coupling of brain glucose metabolism and glutamatergic neuronal activity. *Proc Natl Acad Sci U S A* 95:316–321

Siegel DP (1993) Energetics of intermediates in membrane fusion: comparison of stalk and inverted micellar intermediate mechanisms. *Biophys J* 65:2124–2140

Siesjö B (1978) *Brain energy metabolism.* New York: Wiley

Silver RA, Traynelis SF, Cull-Candy SG (1992) Rapid time course miniature and evoked excitatory currents at cerebellar synapses *in situ*. *Nature* 355:163–166

Silver RA, Cull-Candy SG, Takahashi T (1996*a*) Non-NMDA receptor occupancy and open probability at a rat cerebellar synapse with single and multiple release sites. *J Physiol* 494:231–250

Silver RA, Colquhoun D, Cull-Candy SG, Edmonds B (1996*b*) Deactivation and desensitization of non-NMDA receptors in patches and the time course of EPSCs in rat cerebellar granule cells. *J Physiol* 493:167–173

Silver RA, Momiyama A, Cull-Candy SG (1998) Locus of frequency-dependent depression identified with multiple-probability fluctuation analysis at rat climbing fiber-Purkinje cell synapses. *J Physiol* 510:881–902

Sokoloff L (1960) The metabolism of the central nervous system *in vivo*. In: *Handbook of Physiology, Section I, Neurophysiology, vol. 3* (Field J, Magoun HW, Hall VE, eds), Washington D.C.: American Physiological Society, pp 1843–1864

Sokoloff L, Reivich M, Kennedy C, Des Rosiers MH, Patlak CS, Pettigrew KD, Sakurada O, Shinohara M (1977) The [^{14}C]deoxyglucose method for the measurement of local cerebral glucose

utilization: theory, procedure and normal values in the conscious and anesthetized albino rat. *J Neurochem* 28:897–916

Sokoloff L, Takahashi S, Gotoh J, Driscoll BF, Law MJ (1996) Contribution of astroglia to functionally activated energy metabolism. *Dev Neurosci* 18:344–352

Spruston N, Jonas P, Sakmann B (1995) Dendritic glutamate receptor channels in rat hippocampal CA3 and CA1 pyramidal neurons. *J Physiol* 482:325–352

Tamarappoo BK, Raizada MK, Kilberg MS (1997) Identification of a system N-like Na^+-dependent glutamine transport activity in rat brain neurons. *J Neurochem* 68:954–960

Vetter P, Roth A, Häusser M (2001) Action potential propagation in dendrites depends on dendritic morphology. *J Neurophysiol* 85:926–937

Wolosker H, de Souza DO, de Meis L (1996) Regulation of glutamate transport into synaptic vesicles by chloride and proton gradient. *J Biol Chem* 271:11726–11731

Wong-Riley MTT (1989) Cytochrome oxidase: an endogenous metabolic marker for neuronal activity. *Trends Neurosci* 12:94–101

Wong-Riley MTT, Anderson B, Liebl W, Huang Z (1998) Neurochemical organization of the macaque striate cortex: correlation of cytochrome oxidase with Na^+ K^+ ATPase, NADPH-diaphorase, nitric oxide synthetase and N-methyl-D-aspartate receptor subunit I. *Neurosci* 83:1025–1045